Title
Generation of a New Immunodeficient Rat Model of Retinal Degeneration With LSL TdTomato Reporter and TdTomato-Pcp2 Expression.

Journal
Translational vision science & technology, 15(8)

ISSN
2164-2591

Authors
Seiler, Magdalene J
Nguyen, Helios
Endejan, Devan
et al.

Publication Date
2026-08-01

DOI
10.1167/tvst.15.8.24

tvst

Retina

Generation of a New Immunodeficient Rat Model of Retinal Degeneration With LSL TdTomato Reporter and TdTomato-Pcp2 Expression

Magdalene J. Seiler [1–4,*], Helios Nguyen [1,4,*], Devan Endejan[5], Bin Lin [1,4], Guojun Zhao[5], and Lauren Klaskala [5]

[1] Department of Physical Medicine and Rehabilitation, Sue and Bill Stem Cell Research Center, University of California, Irvine, CA, USA
[2] Department of Ophthalmology and Visual Sciences, Gavin Herbert Eye Institute, University of California, Irvine, CA, USA
[3] Department of Anatomy and Neurobiology, University of California, Irvine, CA, USA
[4] Brunson Center for Translational Vision Research, University of California, Irvine, CA, USA
[5] Inotiv, Maryland Heights, MO, USA

Correspondence: Magdalene Seiler, University of California – Irvine, 845 Health Sciences Rd., 2035 Gross Hall, Irvine, CA 92697, USA. e-mail: mseiler@uci.edu

Received: March 9, 2026
Accepted: July 18, 2026
Published: August 25, 2026

Keywords: photoreceptor degeneration; transgenic rat; cre-recombinase; cre-lox cell label; bipolar cells

Citation: Seiler MJ, Nguyen H, Endejan D, Lin B, Zhao G, Klaskala L. Generation of a new immunodeficient rat model of retinal degeneration with LSL TdTomato reporter and TdTomato-Pcp2 expression. Transl Vis Sci Technol. 2026;15(8):24, https://doi.org/10.1167/tvst.15.8.24

Purpose: The purpose of this study was to develop a fluorescently labeled immunodeficient retinal degenerate (RD) rat model for studying photoreceptor degeneration and transplant-host connectivity using the *Cre-lox* system.

Methods: We developed gene constructs for *CAG-LSL-TdTomato* (expressing floxed TdTomato) and *Pcp2-Cre* (marker for ON-bipolar cells) that were injected into rat embryos. The LSL TdTomato reporter strain, created on immunodeficient *RhoS334ter-3* rats (RRRC #539), was bred to homozygosity (strain *SD-Foxn1rnuTg((Rho-S334X)3,CAG-TdTomato)1010Mjsuc*, RRRC #1055, "RNT"). The gene construct *Pcp2-Cre* was injected into Long-Evans (LE) rat embryos, resulting in two *Pcp2-cre* founders (strain *PCP2 Cre-1105 RKI,* "Pcp2"), with targeted and targeted/random insertion of the transgene. F1 offspring were bred to homozygosity and immunodeficiency. To test whether TdTomato expression can be induced in "RNT" rats expressing floxed TdTomato, retinal explants of P9 "RNT" rats were exposed to AAV-PHP.eB-hSyn-myc-Cre (*AAV-Syn-Cre*) virus. Homozygous rats of both strains ("RNT" and *Pcp2-Cre*) were crossbred to generate *RD TdTomato-Pcp2* ("RTP") rats. Retinas were stained for various retinal markers. GFP-expressing rat retinas were transplanted to 6-week-old "RTP" rats and analyzed after 37 and 77 days.

Results: *AAV-Syn-Cre* induced TdTomato expression in "RNT" retinas. *TdTomato-Pcp2* RD rats developed RD similar to the original *Rho S334ter-3* rats. Retinas with targeted *Pcp2-Cre* insertion showed TdTomato in retinal interneurons, overlapping with Pcp2-staining ON bipolar cells, and cones. Retinas with random *Pcp2-Cre* insertion exhibited additional TdTomato in many other cells. *Pcp2-TdTomato* expression defined transplant-host boundaries.

Conclusions: We created a unique RD rat model for studying retinal transplant connectivity which can also be used to generate RD rats with other cell-specific labels.

Translational Relevance: This newly created rat is useful for cell therapy and retinal degeneration studies.

Introduction

Retinal degeneration (RD), characterized by the progressive loss of photoreceptors and other retinal neurons, comprises a variety of inherited and acquired disorders, such as retinitis pigmentosa (RP)[1,2] or age-related macular degeneration (AMD),[3,4] leading to irreversible visual impairment and ultimately blindness. These conditions affect millions of people in the United

States across different ages and disease prognosis stages, yet effective treatments remain limited. Current treatments including nutritional supplements[3,5] to slow down the progression of RD, do not aim to replace lost photoreceptors. There are also cell therapies already in clinical trials aiming to slow down photoreceptor loss.[6] Our research targets advanced RD when photoreceptor replacement is necessary.

Animal models have played a major role in elucidating the molecular and cellular mechanisms underlying RD and in advancing therapeutic strategies, including gene therapy, pharmacological interventions, and cell replacement (for a recent review, see Ref. 7). Although numerous mouse models have been developed to mimic specific genetic mutations and pathological features of human retinal diseases, rat models offer distinct advantages due to their larger ocular anatomy, relatively easier surgical manipulation, and longitudinal imaging studies.[8–10] However, the availability of well-characterized rat models for RD remains limited, so further studies and experiments are needed to better fit the research purposes and schemes. Rats have advantages over mice in terms of surgical accessibility (larger eyes) and behavioral testing.

Recent advances in regenerative medicine have opened new avenues for therapeutic intervention, with retinal organoid transplantation emerging as a particularly promising strategy.[11–19] Retinal organoids are three-dimensional, self-organizing structures that are derived from human pluripotent stem cells capable of recapitulating key features of the human retina, including photoreceptors and retinal interneurons.[20–22] Transplantation of human retinal organoids into degenerated retinas has shown encouraging results in preclinical models, demonstrating the restoration of visual function to some degree, and offers a renewable source for retinal repair.[14,16–19,23] However, to analyze whether visual improvements by retinal transplants are due to synaptic connectivity between transplant and host retina, it is necessary to unequivocally identify host neurons involved in connectivity.

In this study, we describe the development and characterization of a novel immunodeficient rat model of RD. With the emerging genetic engineering advancement, we used the Cre-loxP recombination system to create a novel transgenic hybrid rat model containing TdTomato-fluorescent retinal bipolar cells. TdTomato was chosen because most donor cells for transplants are labeled with GFP. We created a retinal degenerate strain universally expressing rRosa-*CAG-LSL-TdTomato*, and another strain, expressing *Pcp2-cre* on a Long-Evans (LE) background that was crossed with nude rats to make it immunodeficient. *Pcp2* was expected to label the rod bipolar cells, as has been shown in a mouse model[24,25] and is considered a general marker for retinal ON bipolar cells.[26] After crossing both rat strains, the F1 offspring would be either nude (*foxn1*$^{-/-}$) or non-nude (immunocompetent *foxn1*$^{+/-}$), whereas everyone will possess the transgenic fluorescent retinal component (*TdT-Pcp2*) and exhibit RD. Our findings establish this new model as a valuable tool for advancing the understanding of the retinal connectivity between the transplant and host retinal architecture, which will be valuable for the efficiency and feasibility of retinal transplantation as a novel therapeutic approach.

Methods

Experimental Animals (University of California, Irvine and Envigo)

Animals were treated in accordance with NIH guidelines for the care and use of laboratory animals, the ARVO Statement for the Use of Animals in Ophthalmic and Vision Research, and under a protocol approved by the Institutional Animal Care and Use Committee of University of California, Irvine (UCI). Twenty-four female and 10 male rats of the immunodeficient RD *Rho S334ter-3* rat strain *(SD-Foxn1 Tg(S334ter)3Lav)* were shipped to Envigo (Maryland Heights, MO) in March 2022. At Envigo, fertilized embryos were injected with gene constructs at the one-cell stage and implanted into pseudo-pregnant female rats. After identifying a transgenic founder, the F1 generation of the *TdTomato-1010* rats (RD Nude TdTomato [RNT] rats) was received in April 2023. *Pcp2-Cre* rats were generated on a LE background after embryo injections into immunodeficient *RhoS334ter-3* rats failed. The F1 generation of the *Pcp2-Cre 1105* rats was received in March 2024 (bred with LE and NIH nude rats). Both rat strains were bred to homozygosity at UCI. Homozygous rats of both strains were bred to produce retinal degenerate TdTomato-expressing RD TdTomato-Pcp2 (RTP) rats starting in September 2024. Some RTP rats were processed for immunohistochemistry at different ages, starting at postnatal day (P) 19.

Several of these RTP rats received transplants of rat E19 fetal retinal sheets, derived from a GFP-expressing rat donor (RRRC strain #307) crossed with hPAP *(ACI-Tg(R26_hPLAP)* rats.

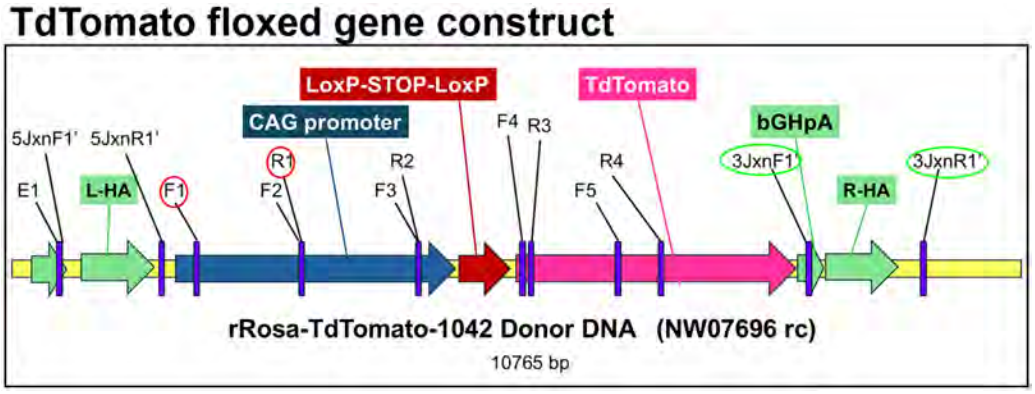

Figure 1. Generation of gene construct for *CAG-LSL-TdTomato* transgene. ZFN engineering was used to create the rROSA-TdTomato-1042 model, with donor DNA (CAG promoter, LSL TdTomato reporter, separated by a LoxP-STOP-LoxP sequence). Schematic diagram of gene construct (5′→3′) with sites of primers indicated (*purple lines*) (see also Table 1 for primers, and Supplementary Table S1 for sequence). Primers shown in Supplementary Figures S1A and S1B are *circled* in *red* and *green*. The primers for random integration screen (3′ BB F/3′ BB R; 5′ BB F/5′ BB R) are not indicated.

DNA Donor Construction for *TdTomato-1010* and Pcp2 (Envigo)

Use of Zinc Finger Nuclease to Create TdTomato-loxP

To generate the CAG-LSL-TdTomato construct, the TdTomato was combined with the CAG promoter. Zinc finger nuclease (ZFN) engineering was used to create the rROSA-TdTomato-1042 model, with donor DNA (CAG promoter, LSL-TdTomato reporter; *TdTomato1010* construct). ZFN bound to the region of interest on the DNA sequence and introduced DNA double strand breaks (DSBs). These DSBs underwent natural cellular reparation, via either error-prone nonhomologous end joining (NHEJ) or high-fidelity homologous recombination (HR) with the provided donor DNA. Each ZFN pair was validated by transfection into cultured rat C6 cells, and cutting efficiency assessed by the Surveyor Cel-1 Mutation Detection assay. The two smaller cleavage bands add up to the size of the parental band. The ratio of the intensity of the cleavage bands relative to the parental band is how we assessed cutting efficiency. Figure 1 shows the gene construct and the sites for the primers used for genotyping (primers see Table 1; base pair [bp] sequence in Supplementary File S1).

The validated gene constructs were then injected into 156 pronuclear embryos of RRRC strain #539.[10] One donor was identified and backcrossed to the original strain (genotyping results in Supplementary Figs. S1A–S1C).

TdTomato1010 Primers (see Table 1): Initial pairings of F1/R1, F2/R2, F3/R3, F4/R4, and F5/R5 primers were used to identify donor (transgene DNA) integration (Supplementary Fig. S1A); 5jxn F/5jxn R to identify targeted gene integration on the 5′ side; 3jxn F/3jxn R to identify targeted integration on the 3′ side (see Supplementary Fig. S1B). Potential founders were screened for random gene integration using the primers 3BB F1′/3BB R1′ and 5BB F1′/5BB R1′ (see Supplementary Fig. S1C).

CRISPR-Cas9 for Pcp2-Cre

The design of the gene construct is shown in Figure 2 (bp sequence in Supplementary Fig. S2). The gRNAs, donor material, Cas9 mRNA, injection buffer, and Cas9 protein (−20°C) were thawed on ice. The gRNAs were lightly vortexed and centrifuged for 2 minutes at 15,000×*g* at 4°C. In a low-binding 0.5-mL microfuge tube, an appropriate amount of gRNAs, Cas9 protein, and Cas9 mRNA were combined, allowing gRNA and Cas9 protein to complex at room temperature for 15 minutes. A cocktail of DNA donors, Cas9 mRNA, and injection buffer was centrifuged for 10 minutes at 4°C at 14,000 RPM. Roughly 20 µL was removed from the top of the mixture without disturbing the bottom and placed in a new tube without creating bubbles. This 20 µL aliquot was used for pronuclear embryo microinjection.

Validation of the Targeting Reagents

Using primers flanking the target site, both the modified and wild-type (WT) sequences were subjected to polymerase chain reaction (PCR) for amplification. The cycle settings allowed the molecules to form both homo and heteroduplexes. Cel-1 endonuclease was utilized to detect heteroduplex and cleaved the mismatched sequences. The digested products were resolved by gel electrophoresis. Primer sequences are listed in Table 1 (*TdTomato-1010*) and Table 2 (*Pcp2-Cre-1105*).

Table 1. rRosa-*CAG-LSL-TdTomato 1010* Primers

Gene Target	Sequence (5′ – 3′)	Expected Band, bp
Donor integration	F1: ACG CCA ATA GGG ACT TTC CA	588
	R1: CGC TCA CCT GTG GGA GTA AC	
	F2: CTG ACT GAC CGC GTT ACT CC	682
	R2: TCC GCA CAG ATT TGG GAC AA	
	F3: ATG GTA ATC GTG CGA GAG GG	875
	R3: GAT GAC CTC CTC TCC CTT GC	
	F4: AGC ATG GAC GTC ATA ACT TCGT	690
	R4: GTG TAG TCC TCG TTG TGG GAG	
	NEW F5: ACA TGG CCG TCA TCA AAG AG	805
	New R5: AGG AAA GGA CAG TGG GAG TG	
ZFN Cel-1/WT, zygosity: HOM should not express it	ZFN-Cel-1 F: GGC GGA TCA CAA GCA ATA AT	395
	ZFN-Cel-1 R: CAG TGG AGT AGG CGG AGA AA	
Rosa Cel-1, zygosity: HOM should not express it	RosaCel-1F: TAA AAT TTG GGT GGG CAT GT	588
	RosaCel-1R: CTG CCT CCT GTC TTC TGA GG	
Target integration	3jxn F1: ATT GCA TCG CAT TGT CTG AG	1354
	3jxn R1: GCC AGT CCA AGA GAA AGC AC	
	5JXN F1: CAG AGA GCC TCG GCT AGG TA	1227 bp
	5JXN R1: GAC GTG AAG AAT GTG CGA GA	
	NEW 5JXN F: CCT CAG AGA GCC TCG GCT AGG TA	1323
	NEW 5JXN R: CGC AAG GAA CCT TCC CGA CTT AG	
Random integration	3′ BB F: TTC CAC ACT TGG GCC TAT TC	~900
	3′ BB R: AGT CGT GTC TTA CCG GGT TG	
	5′ BB F: GTT TTC CCA GTC ACG ACG TT	~750
	5′ BB R: ACT CCA CTG CAG CTC CCT TA	

List of primer pairs used for *TdTomato-1010* genotyping (primers designed by Envigo).

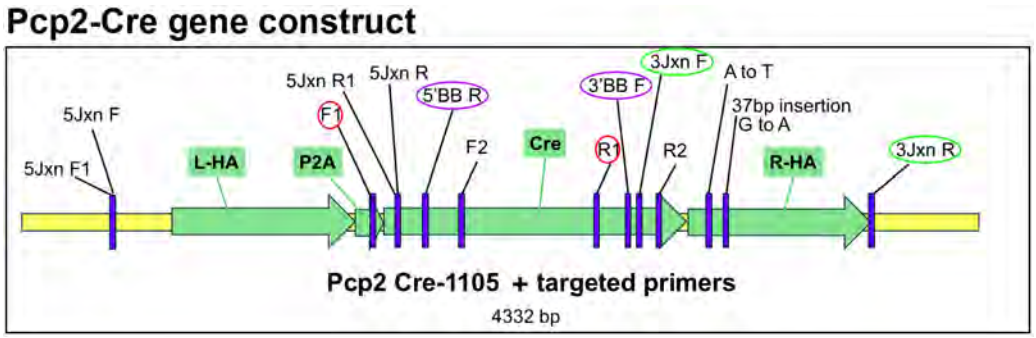

Figure 2. **Generation of Pcp2-Cre gene construct**. CRISPR-Cas9 engineering was to create the *Pcp2 Cre1105* donor DNA. Diagram for Pcp2 Cre-1105 gene construct (5′→3′) with targeted primers (see also Table 2 for primers, and Supplementary Table S2 for sequence). The gene construct for Cre-recombinase (Cre) is flanked by the left homology arm for Pcp2 (L-HA) and a P2A sequence[40] and the right homology arm for Pcp2 (R-HA). Primers shown in Supplementary Figures S2A and S2B are *circled* in *red* and *green*. Only two primers for random integration screen (3′ BB F; 5′ BB R) are indicated (*purple circles*).

Genotyping

DNA Extraction

Tail tissues were collected at the same time as tattooing during neonatal period (P5–P7). Tissues were preserved at −80°C until ready to be extracted. The DNA extraction method followed the protocol provided by the GenCatch Blood and Tissue Genomic Mini Prep Kit (Epoch Life Science).

Table 2. Pcp2-Cre Primers

Gene Target	Sequence (5′ – 3′)	Expected Band, bp
Donor integration screen	Pcp2 F1: AGA ACC CTG GAC CTA TGG CA	650
	Pcp2 R1: AAC CAG CGT TTT CGT TCT GC	
	Pcp2 F2: CGC GGT CTG GCA GTA AAA AC	697
	Pcp2 R2: ACC GGA GAT CAT GCA AGC TG	
Pcp2-Cre Cel-1/WT (zygosity: HOM should not express it)	Pcp2 Cel-1 F: GGT GGC TTC AAA CTC GAG AA	502
	Pcp2 Cel-1 R: ACA GAA GAT CCG GAA GCA GA	
Targeted integration screen	3′ JXN F: TAC GGC GCT AAG GAT GAC TC	1037
	3′ JXN R: TTG TTC CAC AGA GGG AGC TG	
	5JXN F-PCP2: 5′- TCC CGG TGT AGC TGG TGT A	1253
	5JXN R-PCP2: 5′- CGA CCG GTA ATG CAG GCA A	
	5JXN F1-PCP2: 5′- GAT GTC CAG ACA ACC CGT GG	1280
	5JXN R1-PCP2: 5′- CGA CCG GTA ATG CAG GCA AA	
Random integration screen	5′ BB F (Random): GGA GAA AAT ACC GCA TCA GG	1200
	5′ BB R (Random): GCA AAC GGA CAG AAG CAT TT	
	3′ BB F (Random): 5′- CCA CCA GCC AGC TAT CAA CT	900
	3′ BB R (Random): 5′- ATT AGG CAC CCC AGG CTT TA	

List of primer pairs used for Pcp2-Cre genotyping (primers designed by Envigo).

Tissues were incubated with proteinase K in lysis buffer at 60°C for approximately 3 hours. Nucleic acid contents were precipitated by absolute ethanol at room temperature. The mixture was then washed with washing buffer and centrifuged at 8000 RPM for 2 minutes to remove the organic contents and ethanol residues. Preheated Tris-EDTA (TE) buffer (pH 8.0) was used to elute the DNA content. The eluted DNA was stored at −20°C until ready to be amplified.

PCR and Gel Electrophoresis

DNA vials were thawed and kept on ice. Measurements of nucleic acid and protein concentration was performed by Thermo Scientific NanoDrop 2000/2000c Spectrophotometer using a volume of 1 µL for each sample. Each PCR reaction cocktail contained 12.5 µL of the 1X repliQa HiFi ToughMix (Quantabio) master mix ($MgCl_2$, dNTPs, proprietarily formulated HiFi polymerase, hot start antibodies, and ToughMix chemistry), 1 µL of 400 nM each of Forward and Reverse primers, 50 ng of DNA templates, and corresponding RNAse-free water that added up to a total of 25 µL per vial.

PCR reactions were run on Eppendorf Mastercycler (Eppendorf) following these thermal conditions for 35 cycles: initial denaturation at 95°C for 2 minutes, denaturation 95°C for 45 seconds, annealing at 60°C for 1 minute, extension at 72°C for 2 minutes, final extension at 72°C for 5 minutes, and holding at 4°C indefinitely.

Table 3. Determining Zygosity of *TdTomato-1010* or *Pcp2-Cre* Rats

	Primer	
Genotype	ZFN-Cel-1 F/R (TdTomato1010) or Pcp2-Cre Cel-1 F/R (Pcp2-Cre)	Donor Integration
WT	+	–
HET	+	+
HOM	–	+

Schematic table to distinguish heterozygotes (HET) and homozygotes (HOM) from wildtype (WT, no transgene) (primers designed by Envigo).

Samples were resolved on 2% agarose gel (TopVision Agarose; Thermo Scientific) and 1X GelRed Nucleic Acid Stain (Biotium). Gel was visualized under the UV light using the ChemiDoc XRS+ Imager (Biorad).

Determination of Zygosity

Table 3 shows the strategy to determine zygosity of rats (this applies both to *rRosa-CAG-LSL-TdTomato* and *Pcp2-Cre*). Essentially, the Cel-1 F/R primer is expressed by WT and heterozygous rats (not by homozygous rats), and donor integration primers are expressed by heterozygous and homozygous transgenic rats.

Induction of TdTomato Label in *CAG-LSL-TdTomato* Retinal Explants by *AAV-Syn-Cre* (Pilot Experiments)

Virus Source

Adeno-associated virus (AAV) vector AAV-PHP.eB-hSyn-myc-Cre (abbreviated as *AAV-Syn-Cre*) was obtained at a stock titer of 1.81×10^{13} genome copies (GCs)/mL in a total volume of 50 µL from the UCI Center for Neural Circuit Mapping. For the retinal explant virus experiment, the stock virus was diluted in Retinal Medium (RM; 1:1 DMEM/F12; Life Technologies catalog #11330-057) and 10% fetal bovine serum (ThermoFisher Scientific catalog #A5670801) to final working concentrations of 5×10^8, 5×10^9, 5×10^{10}, or 5×10^{11} GCs/mL. These final dilutions were applied to the explants accordingly.

Retina Explant Tissue Isolation and Maintenance

Retinas were isolated from two RNT rats (homozygous for the rRosa-*CAG-LSL-tdTomato* gene) on P9. Rat pups were euthanized after injection of an overdose of ketamine/xylazine. Eyes were enucleated after confirming complete anesthesia. Each retina was dissected into four explanted pieces (total of 8 explanted pieces for the virus experiment). Individual explants were transferred to separate wells of a 24-well plate that was prefilled with 1 mL of RM. A Transwell membrane insert was then placed into each well, and the retinal explant was positioned on the upper surface of the membrane. An additional 200 µL of RM was added into the Transwell insert.

After the culture setup was established, explants were infected with the designated virus dilutions. Explants of pup #1 (RNT325) received viral concentrations of 5×10^8, 5×10^9, or 5×10^{10} vgc (two explants received 5×10^{10}). Explants of pups #2 (RNT331) received either no virus (control) or concentrations of 5×10^8, 5×10^9, 5×10^{10}, or 5×10^{11}. Explants were maintained at 37°C in a humidified incubator with 5% CO_2, and half-medium exchange was performed with fresh RM every other day for 8 days. Explants were fixed in 4% paraformaldehyde in 0.1 M Na-phosphate buffer overnight, then washed with 0.1 M Na-phosphate buffer, placed on slides, incubated with DAPI (4′,6-diamidino-2-phenylindole, 50 µg /mL) over several days at 4°C, and then coverslipped with Vectashield mounting media (Vector Labs). Slides were then imaged in a Leica SP8 confocal microscope at 20× magnification.

Transplantation of Rat Fetal Retinal Tissue (Pilot Experiments)

Retinal tissues were harvested from rat embryos derived from rats universally expressing EGFP (RRRC strain #307, (F344-Tg(UBC-EGFP)F455Rrrc[27] crossed with ACI-Tg(R26_hPLAP, RRRC #817) at embryonic day 19 (E19). Tissues were dissected into rectangular retinal sheets (1–1.3 × 0.6 mm) and stored overnight at 4°C in HibernateE medium with B-27 supplements (Thermo Fisher Scientific) and brain-derived neurotrophic factor (BDNF)/glial cell-line derived neurotrophic factor (GDNF)-loaded poly(lactic-co-glycolic) acid (PLGA) microspheres).

Recipient rats (age 6 weeks) were anesthetized with ketamine/xylazine cocktail (37.5 mg/kg ketamine and 5 mg/kg xylazine). The pupil of the surgery eye was dilated with tropicamide (1%, Somerset). Using a sapphire microblade (World Precision Instruments), a small incision was made just behind the pars plana through the sclera, choroid, and retina, followed by a local retinal detachment. Sheets of retinal tissue were loaded into a custom-made implantation tool (US patent #2 159 218)[28] and inserted into the subretinal space. The scleral incision was closed with 10-0 sutures. Immediately afterward, the fundus was examined by a coverslip on the cornea to locate the transplant placement. The surgery eye was then treated with Neomycin and Polymyxin B Sulfates and Bacitracin Zinc B.N.P. triple antibiotic eye ointment (Bausch & Lomb). After injection of Buprenex (0.03 mg/kg) and Antisedan (0.25 mg/kg; MWI Veterinary Supply, Cencora, CA), rats were placed in an incubator and monitored for full recovery before they were returned to the cages.

Optokinetic Testing (Visual Acuity)

Rats homozygous for the rRosa-*CAG-LSL-tdTomato* gene were tested for tracking moving stripes of varying widths in a virtual cylinder (Optokinetic Testing [OKT] apparatus; Cerebral Mechanics, Alberta, Canada) after at least 1 hour of dark adaptation.[28–30] Six different frequencies (= alternating stripe widths; 0.05–0.45 cycles/degree) were tested for 1 minute each in the clockwise and counterclockwise direction, followed by a blank grey screen, as previously described.[19,28] Rats were tested monthly. Videos of the rat's head following the stripe movements were subsequently analyzed in a masked fashion by two independent observers. The best visual acuity of the two same-day tests was used for analysis. If there was a discrepancy between the two observers,

videos were re-analyzed by a third observer. All testers and video-watchers were blinded to the experimental group assignment of rats. Statistical analysis and graphing data were performed in Graphpad (version 11.0).

Tissue Processing and Immunofluorescence Assay

Rats were euthanized according to the AVMA guidelines, either by CO_2 or by ketamine/xylazine overdose, followed by perfusion fixation with chilled 4% paraformaldehyde (PFA) in 0.1 M sodium phosphate buffer for approximately 10 minutes. Eyes were harvested and soaked in 4% PFA overnight after the cornea was removed to maximize tissue preservation. Tissues were washed the next day with 0.1 M sodium phosphate and further dissected until the eye cups were ready to be infiltrated with 30% sucrose and frozen Tissue-Tek OCT Compound (Sakura). Tissues were cut along the dorsal-ventral axis using Leica Cryostat, and mounted on Superfrost Plus slides (Fisher Scientific). Slides were incubated in HistoVT One (Nacalai, 1:10 dilution, 30 minutes at 70°C) for antigen retrieval, washed with 1× phosphate buffered saline (PBS), and blocked with 20% donkey serum for at least 30 minutes at room temperature, followed by the incubation of a cocktail of primary antibodies at 4°C overnight (see Table 4 for antibodies). After several washes with PBS and a second blocking, the slides were incubated for 30 minutes at room temperature with fluorescence tagged secondary antibodies, Alexa Fluor 488 donkey anti-mouse IgG (H+L) and AF647 donkey anti-rabbit IgG (H+L; Jackson ImmunoResearch). After further washing with PBS, the slides were incubated with DAPI (4′6′-diamidino-2-phenylinode hydrochloride) for 30 minutes at room temperature and were coverslipped with Vectashield mounting media (Vector Labs). For Peanut agglutinin (PNA) lectin staining, slides were blocked with carbo-free blocking solution (CFBS; Vector labs, Cat. # CSP-5040-125) containing 3% Triton X-100 (TX), followed by biotinylated PNA (Vector Labs, Cat. # B-1075-5) diluted 1:200 in CFBS without TX at 4°C overnight. After 3× PBS washes, slides were then incubated in DyLight 649 Streptavidin (Vector Labs; Cat. # SA-5649-1; final conc. 5 ug/mL) in CFBS without TX for 1 hour at room temperature, followed by PBS washes. Slides were then stained with DAPI and coverslipped as described above. Slides were imaged using Leica SP8 confocal microscope (Leica Microsystems). Images were extracted using Leica LSX software.

Table 4. Antibodies

Antibody	Species	Specificity	Dilution	Source; Cat. #	RRID
Primary antibodies					
Calbindin	Mouse	Horizontal cells	1:200	Sigma Aldrich	AB_476894
Calretinin	Rabbit	Ganglion and amacrine cells	1:200	Thermo Fisher Scientific	AB_10985167
CRALBP	Mouse	RPE + Müller glia (MG)	1:1000	Abcam	AB_2269474
GFAP	Goat	Astrocytes + MG (reactive)	1:500	Sigma	AB_10603437
Glutamine synthetase	Mouse	Müller glia	1:1000	Transduction Laboratories	AB_2313767
GFP	Chicken	GFP expressing cells	1:500	Aves labs	AB_2307313
Pcp2	Mouse	Cell expressing Pcp2 (ON retinal bipolar cells)	1:50, 1:200, 1:500	Santa Cruz Biotechnology	AB_2158439
PKCα	Mouse	Rod bipolar cells (cytoplasmic)	1:500	Santa Cruz Biotechnology	AB_628142
PKCα	Rabbit	Rod bipolar cells (cytoplasmic)	1:200	Oxford Biochemical	AB_10814191
Recoverin	Rabbit	Photoreceptor (cytoplasmic) + cone bipolar cells (cBPCs)	1:500; 1:1K	Millipore	AB_2253622
Red-green opsin	Rabbit	LM cones	1:200	Millipore	AB_177456
Rhodopsin (Rho4D2)	Mouse	Rod photoreceptor	1:200	Molday (gift)[39]	N/A
Secretagogin	Rabbit	Amacrine + cBPC + horizontal cells (cytoplasmic)	1:200	Cell Signaling Technology	AB_2798371
α-synuclein	Rabbit	Amacrine + ganglion cells (cytoplasmic)	1:100	Cell signaling	AB_1904156
Conjugate	Species	Specific for	Dilution	Supplier	RRID
Secondary antibodies					
Alexa Fluor 488	Donkey	Mouse IgG (H+L)	1:400	Jackson Immuno Research (West Grove, PA)	AB_2340851
Alexa Fluor 647	Donkey	Rabbit IgG (H+L)	1:400	Jackson Immuno Research	AB_2492288

Results

Generation of Immunodeficient rRosa-CAG-LSL-TdTomato Rats With Retinal Degeneration

After injection of 156 pronuclear embryos of RRRC strain #539 with the TdTomato1010 construct, one founder female rat was identified (out of a litter of 10; see Supplementary Figs. S1A–C). A total of 10 animals were screened for the TdTom-loxP transgene using PCR. Results showed a visible band at the expected size of 588 bp F1/R1 primer for rat #5, suggesting that the donor DNA had integrated into the genome ("donor integration"; see Supplementary Fig. S1A). Furthermore, the animal was screened for "targeted integration" and "random integration" of donor DNA, which exhibited positive bands for both at expected size of 1354 bp and 750 bp, respectively (see Supplementary Figs. S1B, S1C).

The animal was designated as founder, and was backcrossed to rhodopsin-mutant immunodeficient WT (RRRC #539) to generate 10 F1 heterozygous progeny at Envigo which were then shipped to UCI and bred to homozygosity. Figure 3 shows an example of a litter of the F8 RNT generation that was all homozygous for rRosa-CAG-LSL-TdTomato.

Gel electrophoresis indicated no visible bands for WT gene screened by ZFN Cel-1 primers (for primers, see Table 1; Fig. 3A) – indicating homozygosity for the transgene – and visibly bright bands for the internal transgene (i.e. donor integration) screened by TdTom int5 primers (see Fig. 3B) at the expected size of 805 bp. These results revealed that these rats successfully expressed the homozygous *rRosa-CAG-LSL-TdTomato* gene sequence. We have continued to maintain homozygous rRosa-CAG-LSL-TdTomato rats. We have submitted this strain (7 nude male rats, age = 71 days; and 19 female rats, age = 27–35 days) to the RRRC, University of Missouri (strain RRRC #1055; strain name: *SD-Foxn1rnuTg((Rho-S334X)3,CAG-tdTomato)1010Mjsuc*).

Visual Test of Rats With *CAG-LSL-TdTomato* Gene Shows Vision Loss Over Time

OKT was used to test the vision of rats homozygous for the *CAG-LSL-TdTomato* gene. As the rats aged, they exhibited a continuous and significant decrease in visual acuity over the age of 4 to 8 months (see Fig. 3C).

Incubation With AAV-Syn-Cre Induces TdTomato Expression in rRosa-CAG-LSL-TdTomato Retinal Explants

In a pilot experiment in collaboration with the UCI viral core, retinal explants of 2 P9 RNT rats (homozygous for the *rRosa-CAG-LSL-TdTomato* gene) were exposed to different virus concentrations (5×10^8 – 5×10^{11} viral genome copies [vgcs]) and cultured for 8 to 9 days to test whether TdTomato can be induced in RNT rats expressing floxed TdTomato. Clear cellular TdTomato expression in retinal neurons was observed at virus additions of 5×10^9, 5×10^{10}, and $5 \times 10e^{11}$ vgcs. No label was observed in control samples, and a virus concentration of 5×10^8 vgc only resulted in a faint label (Supplementary Fig. S3).

Generation of Pcp2-Cre Rats

Envigo designed sgRNAs targeting the stop codon of rat *Pcp2*, and screened for the most active sgRNAs in cultured cells first, then designed and synthesized donor DNA, containing the specified *Pcp2-Cre* mutation (see Fig. 2). This donor DNA along with Cas9/sgRNA reagent was then delivered into fertilized embryos. However, no transgenic founders could be identified after injecting the *Pcp2-Cre* donor DNA in the immunodeficient *Rho-S334ter-3* rat strain (536 embryos). After switching to LE rats, 2 founders were identified after injection of 291 embryos, both with targeted gene integration, but one of the founders also had random gene integration. A total of seven animals were screened for the Pcp2-Cre transgene using PCR. Results showed a visible band at the expected size of 697 bp for rats #4 and #6, suggesting that they were positive for donor integration (see Supplementary Fig. S2A). Furthermore, both animals exhibited positive bands for targeted integration (see Supplementary Fig. S2B). Rat #4 tested negative for the random integration (see Supplementary Fig. S2C), whereas rat #6 exhibited positive bands for both targeted and random integration at expected size of 1037 bp and 750 bp, respectively (see Supplementary Figs. S2B, S2C, see also primers in Table 2).

The animals were designated as founders and were backcrossed to an LE and to an NIH nude rat, respectively, to generate F1 heterozygous progeny at Envigo. The F1 generation was received in 2024 and bred to homozygosity in 2025 at UCI. The current *Pcp2-Cre* rats show both random and targeted gene integration (GI).

Gel electrophoresis resolved a mix of visible bands and no bands for WT gene screened by Pcp2 Cel-1

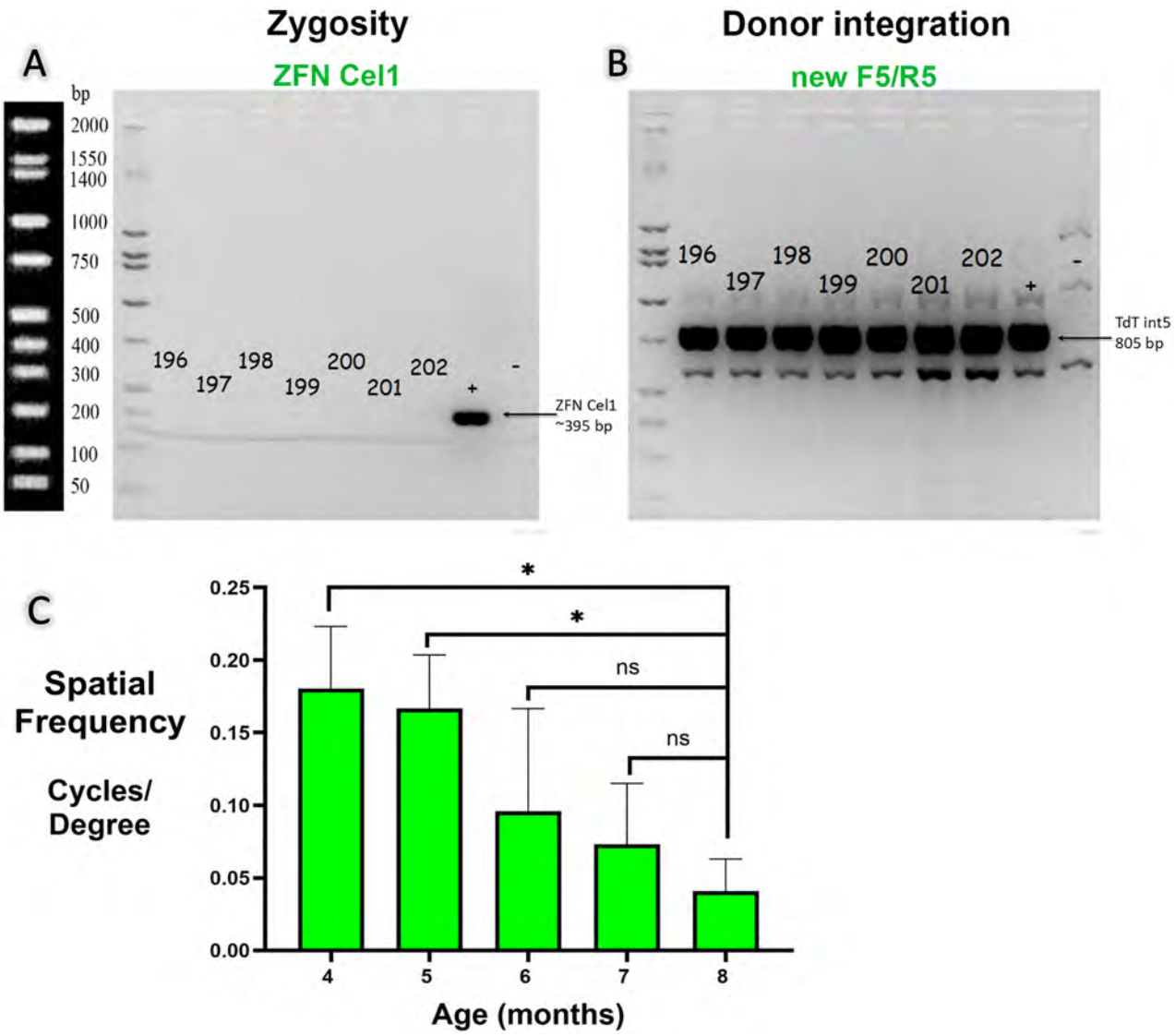

Figure 3. Rats homozygous for the rRosa-CAG-LSL-TdTomato transgene. Genotyping results of TdTomato-1010 litter (F8) generation (all homozygous; see Table 1 for primers). (**A**) ZFN Cel-1 primer for zygosity (only expressed by WT and heterozygotes). (**B**) Donor Integration: all pups express transgene (new F5/R5). (**C**) Optokinetic testing results between the ages of 4 and 8 months ($N = 9$ for 4 and 5 months of age; $N = 3$ for 6 months of age; and $N = 5$ for 7 and 8 months of age). Continuous deterioration of visual acuity. Visual acuity at 8 months is significantly different to visual acuity at 4 and 5 months (unpaired *t*-test with Welch's correction, $P < 0.05$).

primers at 502 bp, and visibly bright bands for the internal Pcp2 transgene screened by Pcp2 int primers at the expected size of approximately 650 bp. Figure 4 shows a litter of the F3 generation, all expressing the *Pcp2-Cre* transgene (positive for F1/R1 int primer; see Fig. 4B). Rats Pcp2-186-195 were homozygous for *Pcp2-Cre* (did not have the Cel-1 primer). Other rats Pcp2-196-198 were positive for the Cel-1 primer, meaning they were heterozygous (see Fig. 4A). These results revealed that the progeny had produced both heterozygous and homozygous *Pcp2-Cre* gene offspring. Rats with the heterozygous *Pcp2-Cre* gene were euthanized, whereas rats with the homozygous *Pcp2-Cre* gene would be conserved and bred to produce successive offspring with the homozygous *Pcp2-Cre* gene.

F1 Offspring of Crossing CAG-LSL-TdTomato and Pcp2-Cre Rats

Homozygous rats of both strains were mated. All rats of the F1 generation were heterozygous for both transgenes (see example in Fig. 5) and expressed TdTomato (Figs. 6–11). Figure 5C shows an example of 4 rats that all showed targeted expression of *Pcp2-*

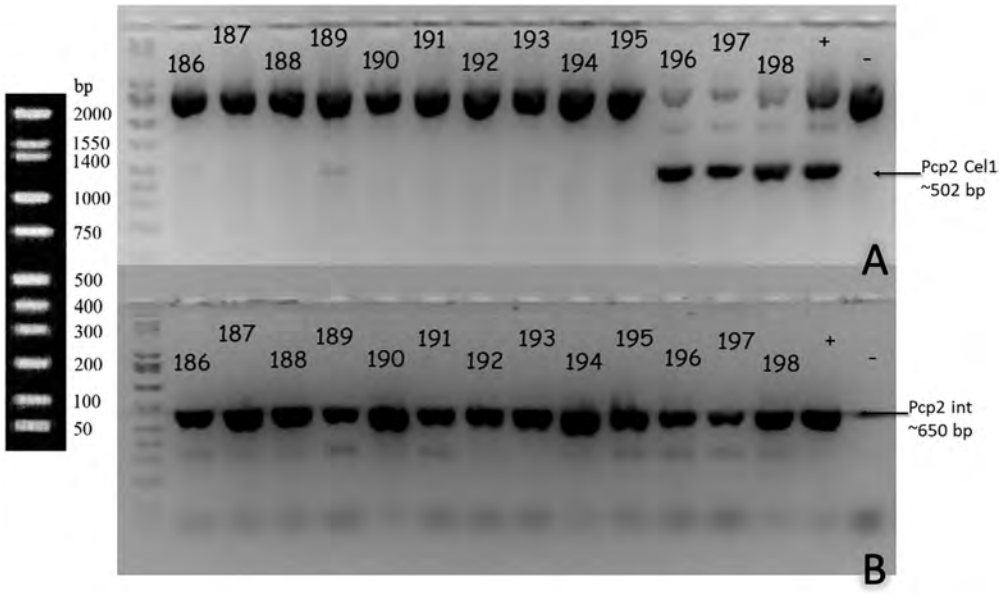

Figure 4. Pcp2-Cre rats of F3 generation (186–198) that are mixed homo- and heterozygous for the transgene. (**A**) Pcp2 Cel-1 primer shows 3 rats expressing the Pcp2 Cel-1 primer (#196–198). (**B**) All rats express at least one copy of the Pcp2-Cre transgene as indicated by the Pcp2 F1/R1 primer (see Table 2 for primers). This means that rats 196 to 198 are heterozygous for the transgene.

Cre (targeted Pcp2-Cre primers), but two of these rats also demonstrated random insertion of the *Pcp2-Cre* transgene (Fig. 5D).

Targeted TdTomato Expression

Animals that were only positive for targeted integration of the *Pcp2-Cre* transgene (examples in Figs. 5C, 5D) expressed TdTomato fluorescent cells in the retina (see Figs. 6A1, 6A2, 6B1, 6B2), specifically in the cone bipolar cells (marker secretagogin) in the inner nuclear layer (INL; see Figs. 6D1, 6D2) in addition to scattered cone photoreceptor cells in the outer nuclear layer (ONL; see Figs. 6, 7A, 7B, 8C–H). Interestingly, there was only limited co-localization with the rod bipolar cells marker PKCα (see Figs. 6C, 7E, 7F), but some colocalization with the horizontal cell marker Calbindin (see Fig. 6C).

Colocalization of TdTomato With Pcp2 in RTP Rats With Targeted TdTomato Expression

Figure 7 shows the comparison of TdTomato expression in the retina with staining for a monoclonal antibody against Pcp2 and the retinal marker recoverin (photoreceptors and cone bipolar cells; see Figs. 7A, 7B), Calretinin (ganglion and amacrine cells; see Figs. 7C, 7D) and PKCα (rod bipolar cells; see Figs. 7E, 7F), at two different ages. Pcp2 mostly overlapped with TdTomato expression. The subpopulation of recoverin-positive and TdTomato-expressing photoreceptors did not stain for Pcp2. Most recoverin-positive cone bipolar cells did not express TdTomato (see Figs. 7A, 7B; see magnification inserts), although some cells were co-labeled (arrows in Figs. 7A, 7B). Some TdTomato-labeled cells were labeled with the Calretinin antibody and were negative for Pcp2 (see Figs. 7C, 7D, arrows). Some cells co-expressing PKCα and TdTomato also expressed Pcp2. However, many PKCα positive cells were not labeled by TdTomato or Pcp2 (see Figs. 7E, 7F).

The time course of photoreceptor degeneration between P19 and 35 is shown in Figure 8, using the markers rhodopsin (see Figs. 8A, 8B), recoverin (see Figs. 8C, 8D), red-green opsin (see Figs. 8E, 8F) and PNA (Figs. 8G, 8H). The ONL was reduced from 2.5 rows to 1 row between P19 and P35. Cones still presented with short outer segments on P19 (see Figs. 8E, 8G) which looked very distorted and abnormal on P35.

Random and Targeted TdTomato Expression

As predicted from the genotype of the F1 RTP rats, animals containing both random and targeted integrated *Pcp2-Cre* transgene (see Figs. 9–11), exhibited both random and targeted TdTomato fluorescent signals in retinal bipolar cells, as well as

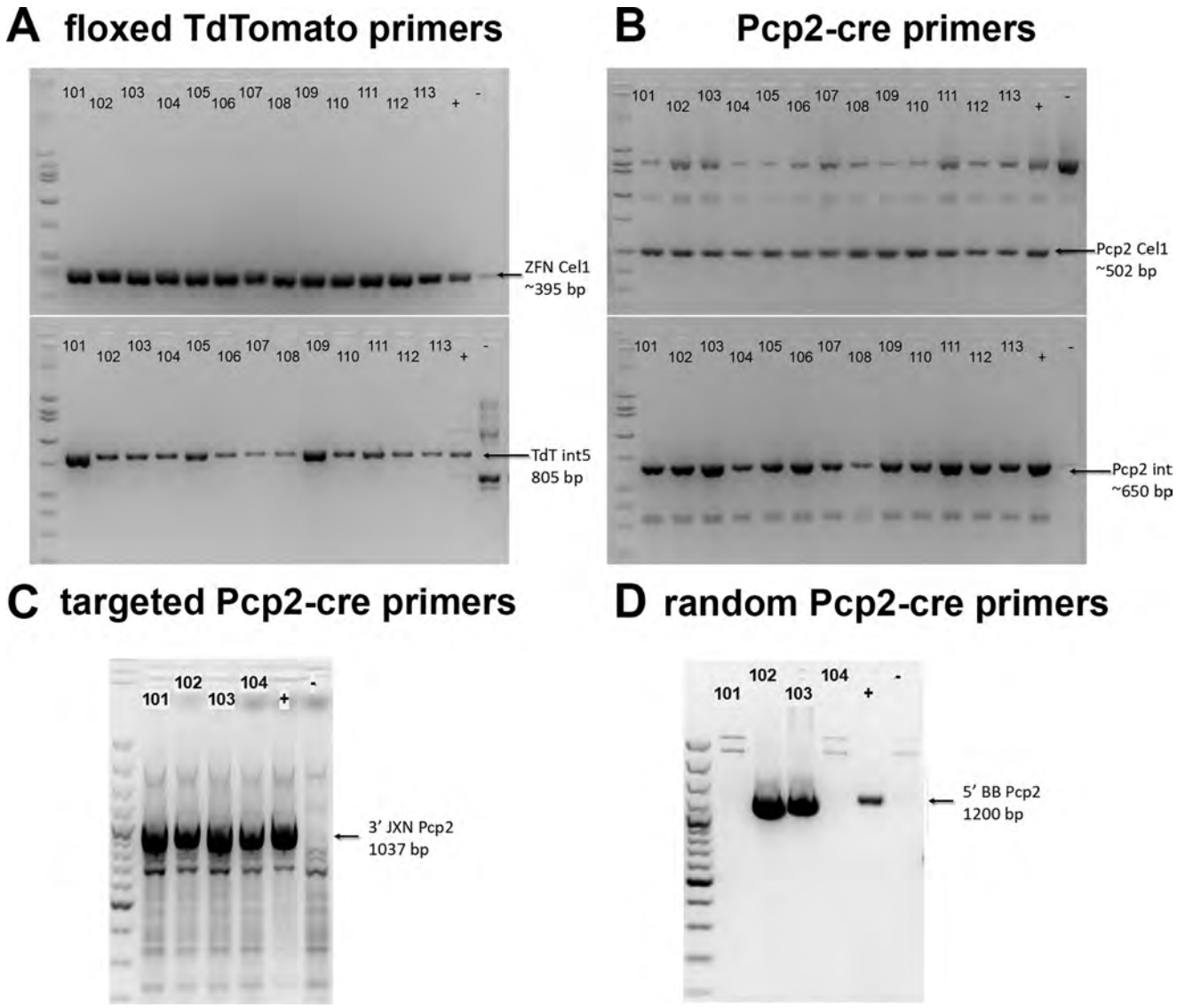

Figure 5. Genotyping results of F1 cross of homozygous rRosa-*CAG-LSL-TdTomato* and homozygous *Pcp2-Cre* rats. All F1 rats (designated "RTP") are heterozygous for *CAG-LSL-TdTomato* and *Pcp2-Cre*. (**A**) Primers ZFN Cel-1 (top, for Zygosity, 395 bp) and CAG-LSL-TdTomato transgene ("TdT int5" = new F5/R5, 805 bp) (see Table 1 for primers). (**B**) Primers Pcp2 Cel-1 (*top*, for zygosity, 502 bp) and Pcp2 integration (Pcp2 int = F1/R1 primer, 650 bp) (see Table 2 for primers). (**C**) "RTP" rats #101–104 are positive for targeted *Pcp2-Cre* primer ("3′ JXN", 1037 bp). (**D**) Two of these rats (RTP #102 and #103) also express the primer for random *Pcp2-Cre* integration ("5′ BB", 1200 bp). RTP #101 and #104 only express the targeted primer (see Table 2 for primers). This is reflected in their TdTomato expression (see Figs. 6–11).

the RPE, Müller glia, and astrocytes and blood vessels/endothelial cells (see Figs. 9A, 9B, 10, 11).

In animals with random/targeted integration of the transgene, a variety of retinal cells from different retinal layers expressed the TdTomato signal along with retinal BPCs. Colocalization of the cytoplasmically stained cells (recoverin) in the ONL with TdTomato-suggested that some cone photoreceptors also arbitrarily expressed the fluorescent signal, whereas, at the same time, recoverin-positive cone bipolar cells from the INL also showed colocalization with the TdTomato-positive cells (see Figs. 10A, 10B, 11C, 11D). Further examination of the INL also showed that the TdTomato signal colocalized with Glutamine synthetase (see Fig. 9D) and CRALBP (Müller glia and RPE; see Figs. 10C, 10D), PKC*α* (rBPCs; see Figs. 9C, 10E, 10F), and secretagogin (cBPCs; see Figs. 9D, 10G, 10H), which suggested that these retinal cells also expressed TdTomato. Photoreceptor degeneration, as shown by rhodopsin, recoverin, RG-opsin, and PNA staining between P19 and P61 was similar in rats with both

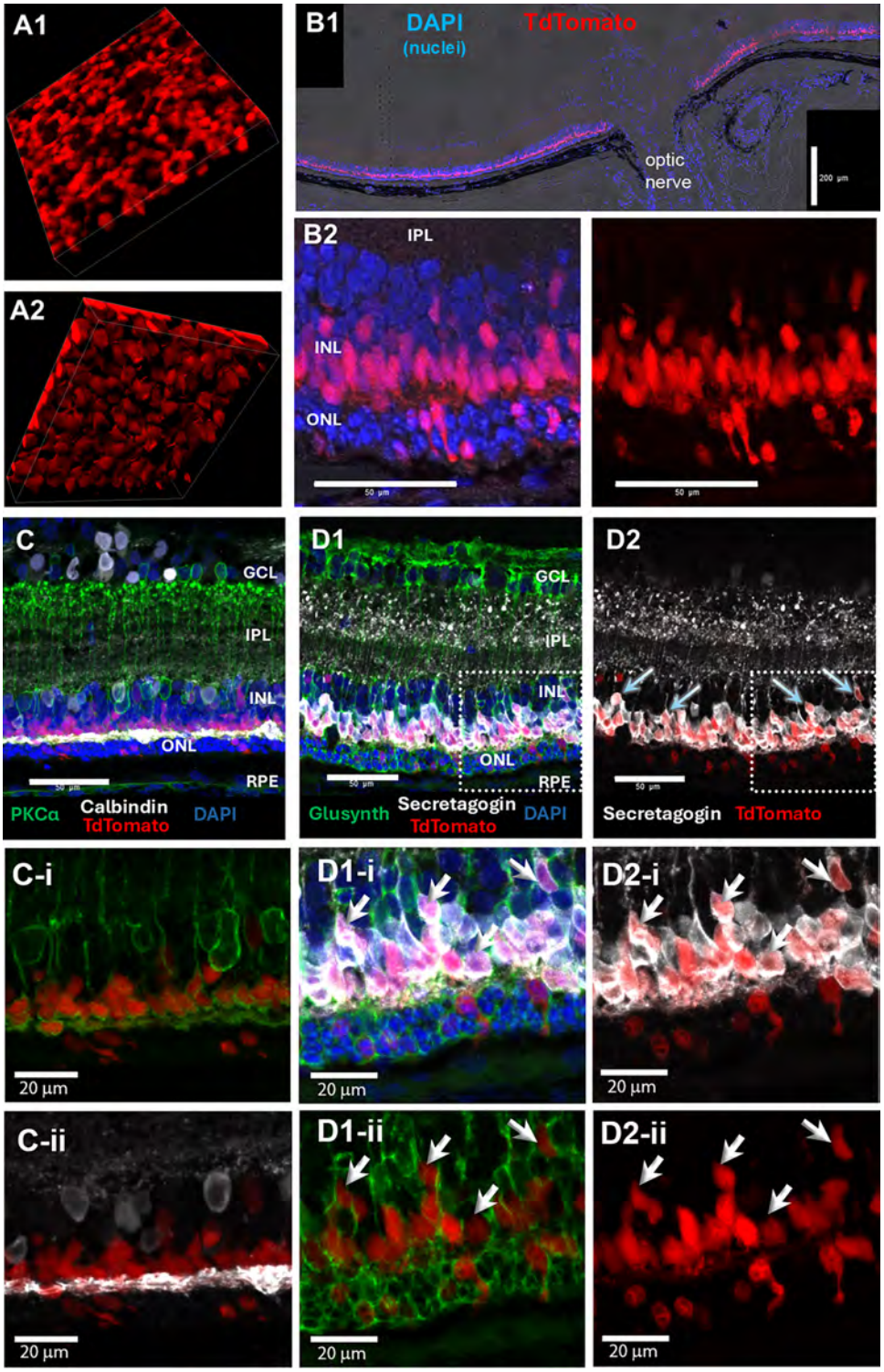

Figure 6. **"RTP" rat with targeted TdTomato expression, postnatal day 19.** (**A**) Retinal wholemount stack seen at different angles. (**B**) Retinal section through optic disk counterstained with DAPI. (**B1**) Overview section through optic disk. (**B2**) Enlargement of different section, showing TdTomato stain in inner nuclear layer and subgroup of photoreceptors. At this age, there is still a thin outer nuclear layer (2–4 nuclei) left. (**C**) PKCα (*green*; rod bipolar cells), Calbindin (*white*; horizontal cells), and TdTomato (*red*). Enlargements: **C–i** (PKCα, TdTomato), **C–ii** (calbindin, TdTomato). Not much overlap between PKCα or Calbindin and TdTomato. (**D**) Glutamine synthetase (*green*; Müller cells), Secretagogin (*white*; cone bipolar cells), and TdTomato (*red*). (**D1**) All channels, including DAPI. White arrows in D1–i, D1–ii, D2–i, and D2–ii indicate examples of double-stained cells for TdTomato and Secretagogin. (**D1–i**) enlargement of box in D1. (**D1–ii**) Enlargement TdTomato, Glutamine synthetase (*green*). (**D2**) Secretagogin (*white*) and TdTomato (*red*). Overlap between TdTomato and Secretagogin in many cells, however, no complete overlap. **(D2–i**) Enlargement of box in D2. (**D2–ii**) Enlargement, TdTomato only. Bars = 200 µm (**B1**), = 50 µm (**B2, C, D1, D2**), = 20 µm (**C–i, C–ii, D1–I, D1–ii, D2–I, D2–ii**).

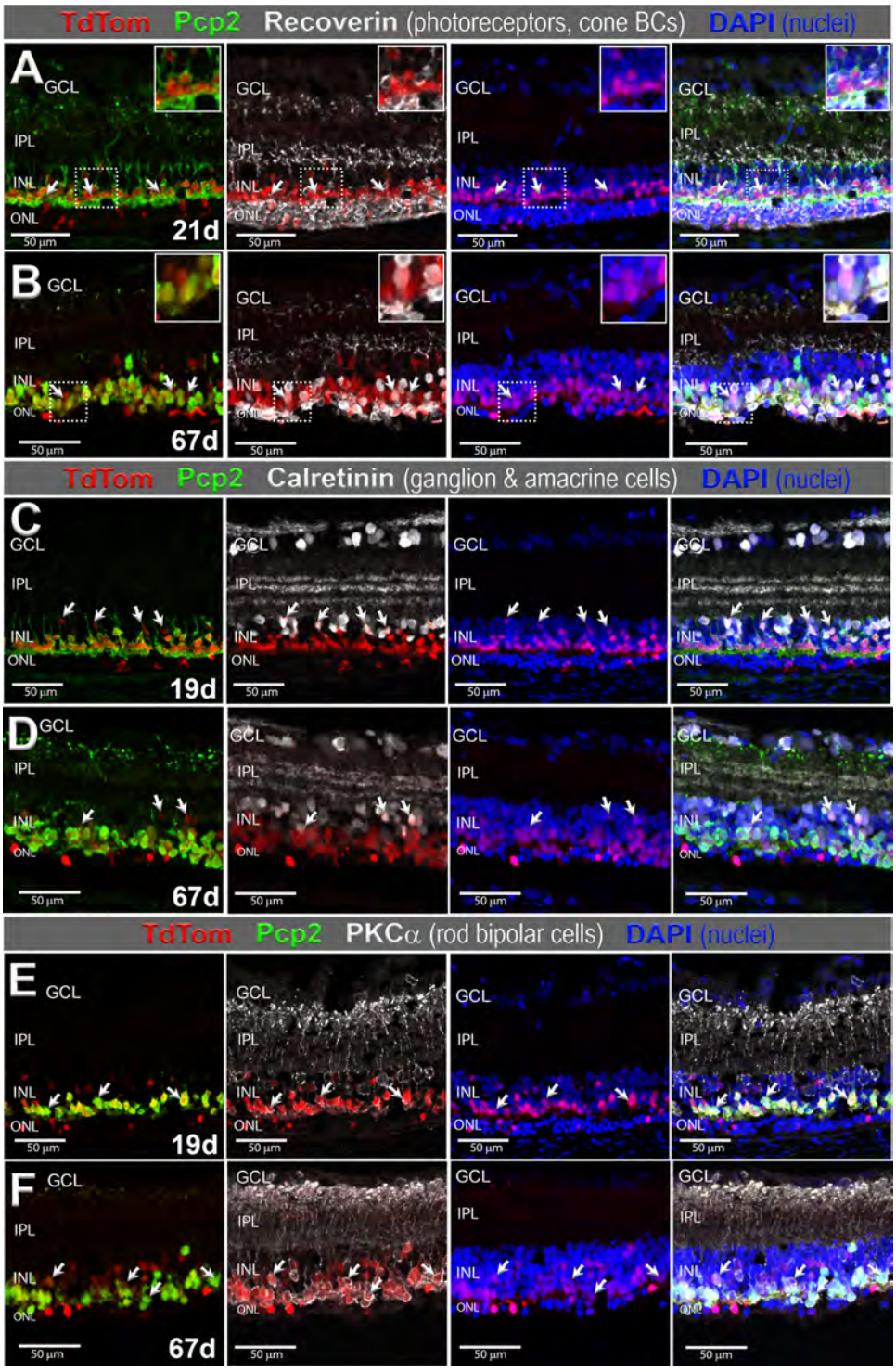

Figure 7. **Comparison of TdTomato and Pcp2 expression (*green*) in "RTP" rats in combination with other retinal markers** (Recoverin, Calretinin, and PKCα; *white*). RTP rats with targeted gene insertion, at age P19 or 21, respectively (**A, C, E**) and **P67** (**B, D, F**). From *left* to *right*: TdTomato/Pcp2 (*green*); TdTomato/rabbit antibody; and TdTomato/DAPI; merged image. TdTomato expression overlaps mostly, but not completely with Pcp2. (**A, C, E**) At 19 or 21 days, there is still a thin outer nuclear layer present, containing some TdTomato-labeled photoreceptors. (**B, D, F**) At 67 days, the outer nuclear layer has mostly disappeared and only few scattered photoreceptors are seen. (**A, B**) Combination with recoverin (photoreceptors and cone bipolar cells). A subpopulation of photoreceptors expresses TdTomato. Note that some recoverin positive cone bipolar cells do not express TdTomato (enlargements in **A** and **B**), and some cells faintly stained for recoverin express TdTomato (*arrows*). In **B**, recoverin-labeled TdTomato+ cells (arrows) do not stain for Pcp2. **C, D** Combination with Calretinin (ganglion and amacrine cells). TdTomato labeled cells positive for Calretinin (*arrows*) do not express Pcp2. **E, F** Combination with PKCα (rod bipolar cells). *Arrows* point to examples of cells co-expressing PKCα and TdTomato. These cells also express Pcp2. However, there are many PKCα-positive cells not labeled by TdTomato or Pcp2. Bars = 50 µm.

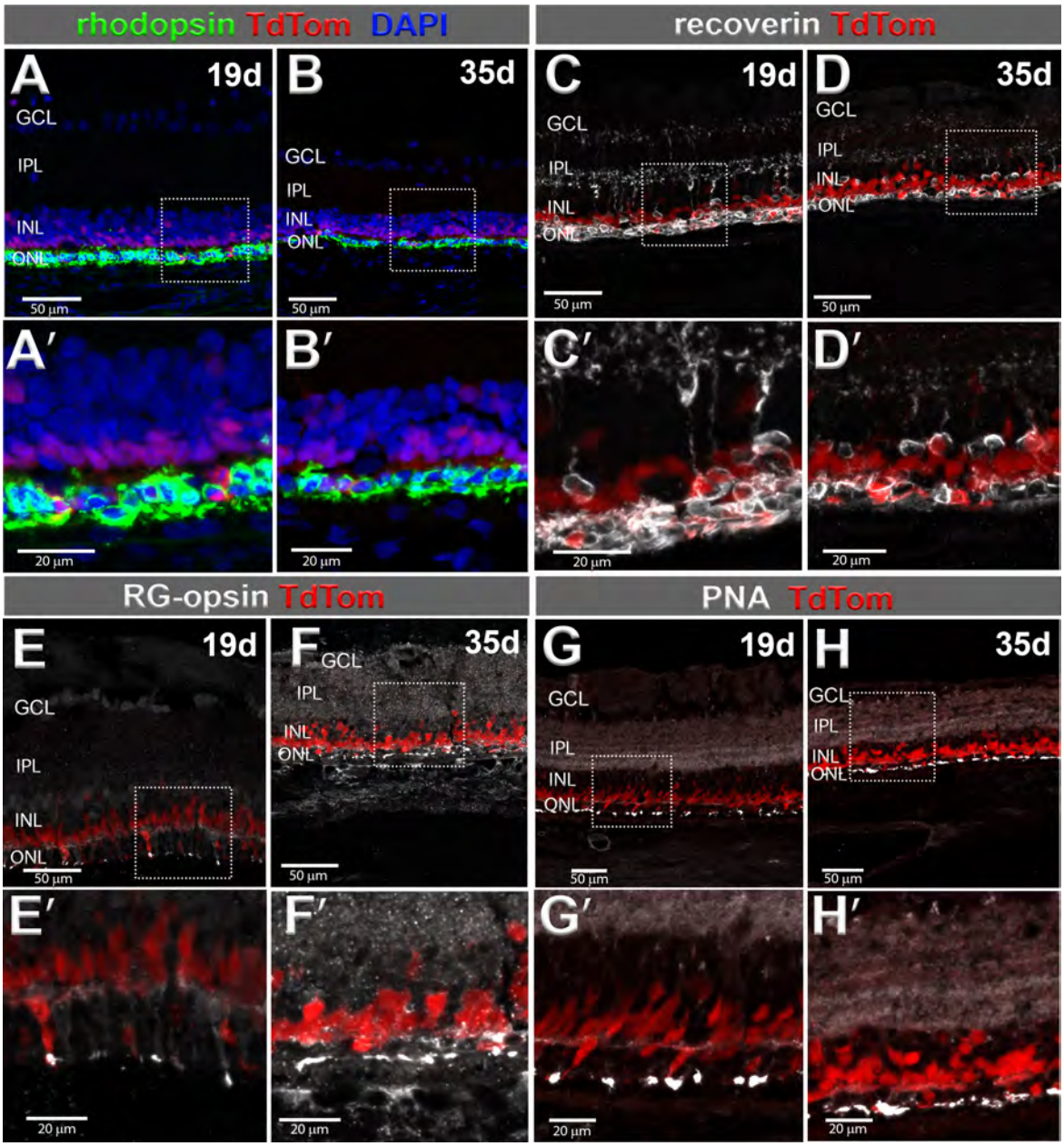

Figure 8. Photoreceptor markers in "RTP" rats with targeted TdTomato expression show progressive photoreceptor degeneration. RTP rats with targeted gene insertion, at 2 different ages (postnatal days [P]19 and 35). All panels show an overview in the top row, and an enlargement (indicated by box) below. (**A, B**) Rhodopsin (*green*). **A** On P19, approximately 2 rows of photoreceptors left. Abnormal rhodopsin staining in cell bodies of rods. Few TdTomato cells in ONL. **B** On day 35, outer nuclear layer is reduced to one row. (**C, D**) Recoverin (marker for photoreceptor and cone bipolar cells; *white*) on P19 **C** and P35 **D**. (**E, F**) Cone red-green opsin staining (*white*) on P19 **E** and P35 **F**. Bars = 50 µm **A** to **H**, = 20 µm (**A′**–**H′**). (**G, H**) Peanut agglutinin (PNA) staining (marker for cone extracellular matrix, white) on P19 **G** and P35 **H**. Note the significant degeneration between P19 and P35.

targeted and random/targeted *Pcp2-cre* expression (see Fig. 11).

Examples of Pilot GFP transplants in TdTomato Host

Figure 12 shows examples of GFP-expressing rat retinal transplants to RTP rats with targeted or targeted/random *Pcp2-Cre* expression. The transplant to a rat with targeted *Pcp2-Cre* expression in Figures 12A and 12B (37 days post-surgery [dps]), contained photoreceptors in a rosette, showed intermingling to transplant and host cells at the transplant host interface, extension of transplant processes into the host INL, and extension of host processes into the transplant. A transplant to a rat with random *Pcp2-Cre*

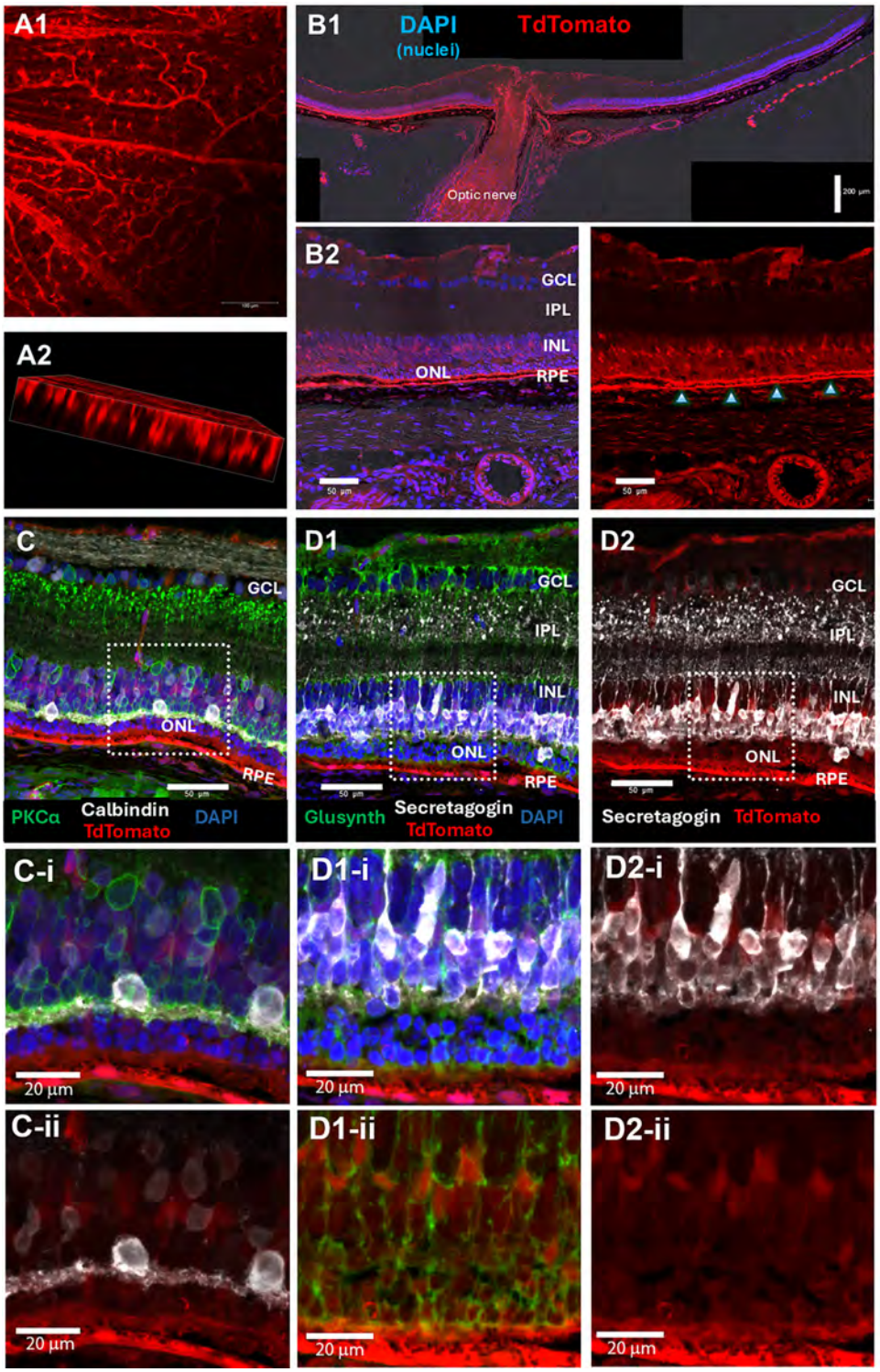

Figure 9. "RTP" rat with random TdTomato expression, postnatal day 19. (**A**) Retinal wholemount stack seen at different angles. (**A1**) Shows blood vessel staining; (**A2**) shows radial cells (Müller glia). (**B**) Retinal section through optic disk counterstained with DAPI. (**B1**) Overview section through optic disk (TdTomato stain in optic disk); (**B2**) enlargement of different section, showing TdTomato stain in inner nuclear layer, but also in the RPE and in blood vessels. (**C**) PKCα (*green*; rod bipolar cells), Calbindin (*white*; horizontal cells), and TdTomato (*red*). (**C–i**) (PKCα, TdTomato), (**C–ii**) (calbindin, TdTomato). Not much overlap between PKCα or Calbindin and TdTomato. (**D**) Glutamine synthetase (*green*; Müller cells), Secretagogin (*white*; cone bipolar cells), and TdTomato (*red*). (**D1**) All channels, including DAPI. (**D1–i**) Enlargement of box in **D1**. (**D1–ii**) Enlargement TdTomato, Glutamine synthetase (*green*). (**D2**) Secretagogin (*white*) and TdTomato (*red*). (**D2–i**) Enlargement of box in **D2**. (**D2–ii**) Enlargement, TdTomato only. Overlap between TdTomato and Secretagogin in subgroup of cells. Note additional TdTomato label in RPE, blood vessels and glial cells. Bars = 200 µm (**B1**), = 50 µm (**B2, C, D1, D2**), = 20 µm (**C–i, C–ii, D1–I, D1–ii, D2–I, D2–ii**).

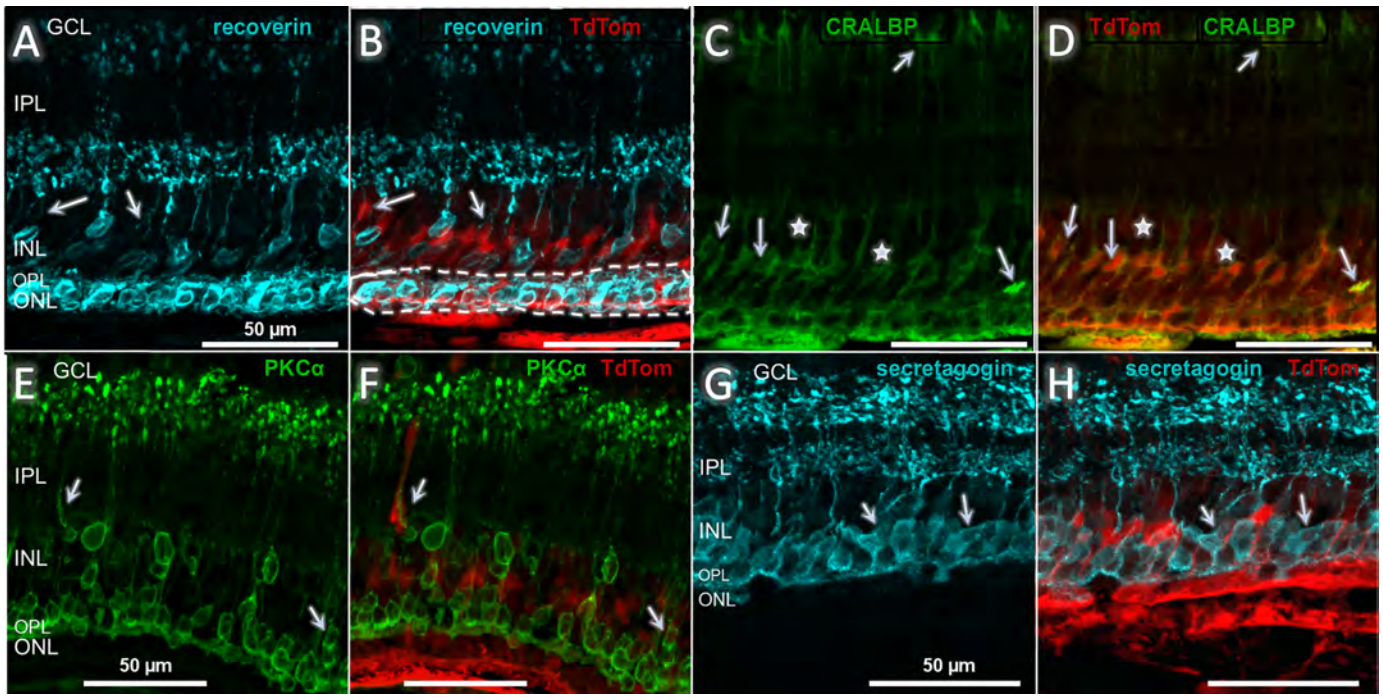

Figure 10. **Staining of "RTP" rats with random TdTomato expression**. Strong TdTomato expression in RPE and radial cells in the retina. (**A, B**) Recoverin (turquoise) on P19. Arrow points to same TdTomato+ cells in **A** and **B**. *Dashed line* in **B** indicates photoreceptor layer. (**C, D**) CRALBP (*green*, Müller glia cells and RPE) on P19 (same section). Several TdTomato+ cells are co-labeled for CRALBP. (**E, F**) PKCα (*green*, rod bipolar cells). *Arrows* indicate TdTomato+ cells co-labeled with PKCα. However, TdTomato-structure labeled on the left side is a blood vessel in close vicinity to a PKCα-labeled process. (**G, H**) Secretagogin (*turquoise*) on P35. In the random Td-Tomato-expressing rat, there is still relatively faint stain of Secretagogin+ cells, but the stronger label appears in Secretagogin-negative cells (presumably Müller cells). Bars = 50 µm.

expression (see Figs. 12C, 12D, 77 dps) had developed a photoreceptor layer with outer segments in contact with host RPE expressing TdTomato. The enlargement showed host cell processes, as well as host-derived blood vessels extending into the transplant. Donor cells had migrated into the host retina (see Fig. 12C).

Discussion

The *Cre-loxP* system is universally useful to create cell type-specific gene expression or label (for review, see Refs. 31, 32). In the current study, we have generated immunodeficient retinal degenerate *RhoS334ter-3* rats expressing a *CAG-LSL-TdTomato* transgene (*TdTomato1010*, RNT, and RRRC strain #1055), When crossed to *cre*-expressing strains, the F1 offspring (RTP) will express TdTomato in *Cre*-expressing cells and show severe RD as the rhodopsin mutation is dominant. We have created immunodeficient *Pcp2-Cre* expressing rats from two founders, both with targeted gene insertion. However, the second founder expressed *Pcp2-Cre* also randomly.

In the RTP rats expressing only targeted *Pcp2-Cre* transgene, most of the TdTomato in the retina overlapped with Pcp2 staining. However, there were additional Pcp2-negative cells expressing TdTomato (subpopulation of cone photoreceptors, and inner retinal cells staining for Calretinin). In contrast to *Pcp2-Cre* mouse models with specific label of rod bipolar cells (labeled by PKCα),[24,25] our rat model with targeted Pcp2-Cre expression showed most of the TdTomato label in cone bipolar cells, not in rod bipolar cells, and in some additional cone photoreceptors. Thus, the function of the *Pcp2* gene may be different between mice and rats.

The creation of this new rat strain can be beneficial to studying RD in several ways. The parents, containing the *Foxn1* gene mutation, as well as the *Pcp2-Cre* or *TdTomato-LoxP*, have produced a generation of a novel hybrid model, where the descendants contain both the *Foxn1* mutation and TdTomato-fluorescent *Pcp2* gene in the retina. Rats with the *Foxn1* gene mutation can be bred to express either non-nude WT (*foxn1*$^{+/-}$), which produces immunocompetence that can be useful for studying allotransplantation in the rat model, or nude, homozy-

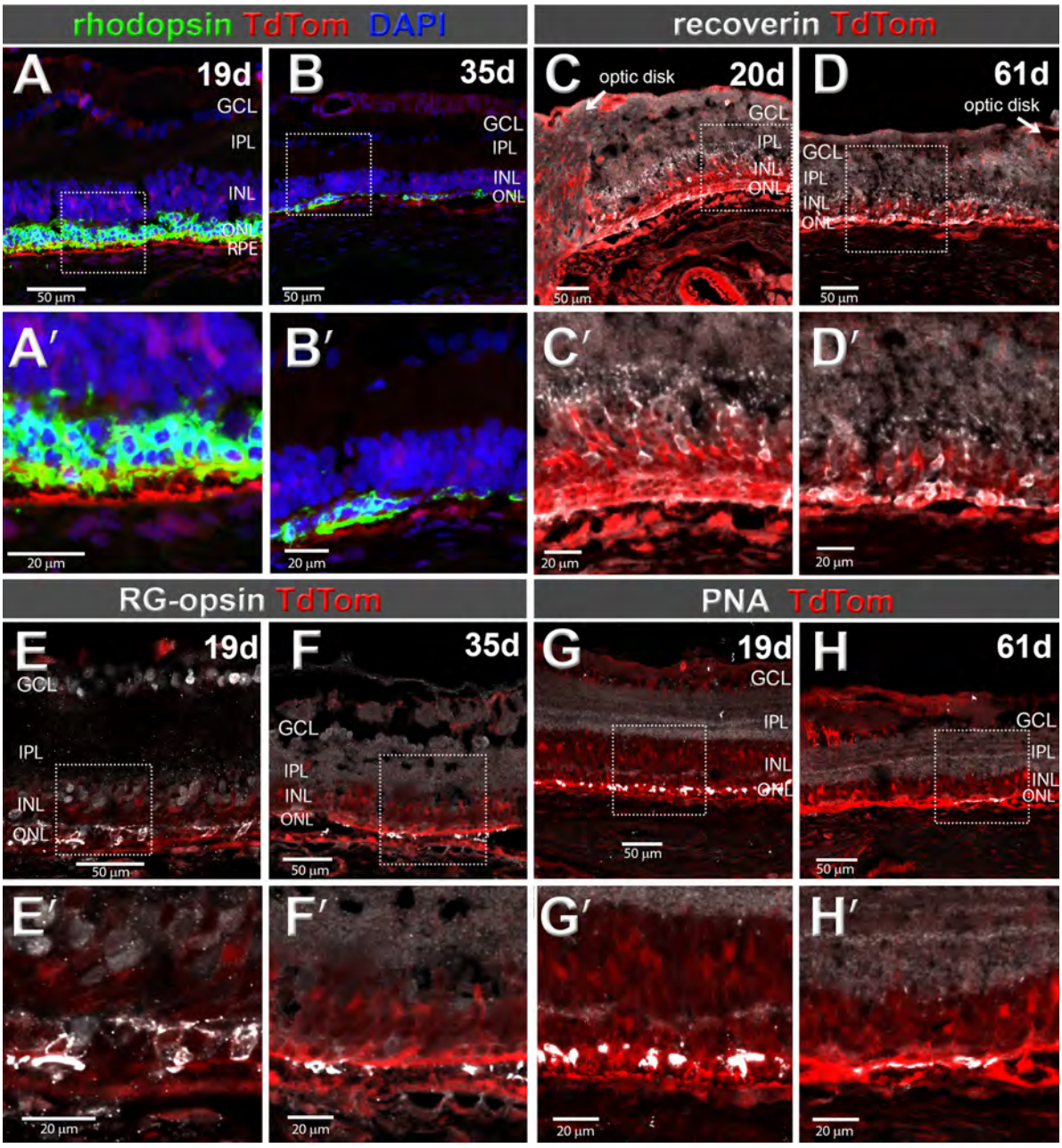

Figure 11. Photoreceptor markers in "RTP" rats with targeted TdTomato expression show progressive photoreceptor degeneration. RTP rats with targeted gene insertion, at two different ages (P19 and P35). All panels show an overview in the top row, and an enlargement (indicated by *box*) below. (**A, B**) Rhodopsin (*green*). **A** On P19, approximately two rows of photoreceptors left. Abnormal rhodopsin staining in cell bodies of rods. Few TdTomato cells in ONL. **B** On P35, outer nuclear layer is reduced to one row. (**C, D**) Recoverin (marker for photoreceptor and cone bipolar cells; *white*) on P19 **C** and P35 **D**. (**E, F**) Cone red-green opsin staining (*white*) on P19 **E** and P35 **F**. Bars = 50 µm (**A–H**), = 20 µm (**A′–H′**). **(G, H**) Peanut agglutinin (PNA) staining (marker for cone extracellular matrix, *white*) on P19 **G** and P35 **H**. Note the extensive photoreceptor degeneration at the age of 61 days.

gous (*Foxn*$^{-/-}$), which exhibits phenotypically immunodeficient characteristics that is suitable for xenotransplantation of the human embryonic stem cell-derived retinal organoid (hESC-RO) to minimize immune rejection.[16,17,19] The hESC-derived retinal organoids can also be successfully transplanted to immunocompetent *Foxn1*$^{+/-}$ recipients with immunosuppression.[15] On the other hand, the creation of cell-specific fluorescent labeling, such as of retinal bipolar cells, has proven the effectiveness and versatility of the *Cre-LoxP* system. Moreover, retinal bipolar cells are an important structure of the retina, which play an important role in

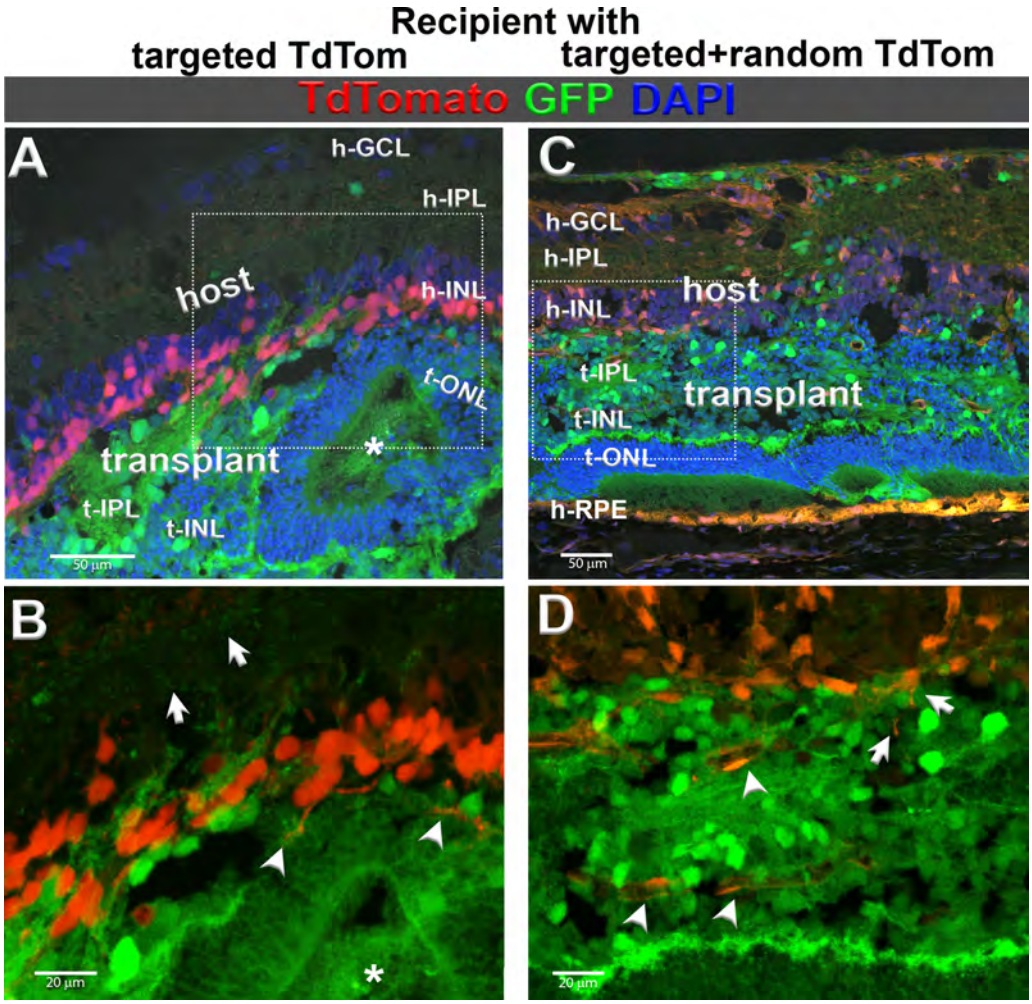

Figure 12. **Td-Tomato-labeled *RhoS334ter-3* recipients ("RTP") with transplants of GFP-expressing rat retinal sheets** (grafted on E19). Sections stained with antibody against EGFP. Top (**A, C**) TdTomato, GFP, and DAPI (nuclei), *boxes* indicate areas of enlargement in bottom (**B, D**) shown with *red* and *green* channels only. **A B** Recipient with targeted TdTomato expression (as described in Figs. 6, 8). **A** Transplant with photoreceptor rosette, lumen indicated by *asterisk*. *Arrows* in the enlargement in **B** point out GFP+ processes in the host inner plexiform layer. *Arrowheads* point to host processes extending into the transplant. (**C, D**) Recipient with random TdTomato expression in a variety of cell types (as described in Figs. 7, 9, 10). **C** Transplant has developed outer nuclear layer, with photoreceptor outer segments toward the host RPE expressing TdTomato. **D** Enlargement. *Arrowheads* point to host-derived, TdTomato expressing blood vessels in transplant. *Arrows* point to cell processes extending into the transplant. Bar in **A** C = 50 µm; Bars in **B D** = 20 µm.

initial signal integration and processing before passing onto high-order visual processing in the central nervous system, and their ability to adapt in RD is an attractive field of vision research. The novel hybrid model, therefore, offers a more comprehensive versatility to further elucidate the molecular basis of RD and how it affects the later components of the retinal circuit, as well as understand the feasibility of hESC-RO in rescuing or delaying the prognosis of RD.

Using the ZFN Cel-1 method, rats were able to acquire the TdTomato gene flanked between the loxP sites. Despite its high affinity, there was still a mix of random and integrated transgene in the animals. However, the effect of random integration of the *loxP* gene was not as severe as seen in that of the *Cre* gene. *CRISPR-Cas9* technology, in spite of its versatility and efficiency, was used to generate a mixed batch of random and targeted integration. Because the *Cre* protein was responsible for dictating which cells would express the TdTomato fluorescent gene, random integration of the *Cre* gene sequence outside of the *Pcp2* promoter site would lead to random TdTomato expression of other cells besides *Pcp2*-expressing cells, as seen in the immunofluorescent results. According to our results, certain ocular structures, such as the RPE, photoreceptors, Müller cells, retinal ganglion cells, and retinal blood vessels, exhibited much stronger TdTomato expression than retinal bipolar cells in

the rats expressing random *Pcp2-Cre*. Some rats also appeared to have pink skin, hair, nails, and lens; therefore, depending on the location of the *Cre* transgene, results may vary, and would not be useful to study specific retinal cell structure, such as the bipolar cells. Therefore, rats should be examined for phenotypically abnormal appearance (pink hair, skin, lens, and transparent RPE) coupled with genotyping to eliminate random TdTomato expression.

There are several issues that make it more difficult to create transgenic rats versus mice. Whereas mouse embryonic stem (ES) cells have been well-characterized and used since the 1980s for gene targeting, stable and pluripotent rat ES cell lines have historically been more difficult to derive and maintain.[33] This has limited the use of homologous recombination for targeted genetic manipulation in rats. Rats have more complex reproductive physiology, making techniques like pronuclear injection and embryo manipulation technically harder and less efficient compared with mice. Rat embryos are more fragile and sensitive to manipulation, which leads to lower survival and integration rates of the foreign DNA. The development and application of gene-editing tools like CRISPR/Cas9 and ZFNs in rats occurred later than in mice. Although this has improved transgenic rat generation in recent years, mice still remain the more accessible and widely used model.

Despite these challenges, transgenic rats have remained a favorable animal model for in vivo study of human diseases such as RP and macular degeneration. Rats possess larger eyes than mice, making them more suitable for ophthalmic intervention and retinal imaging. Rats can also model specific mutations associated with human retinal diseases, making it a valuable tool for in vivo testing of gene therapy, stem cell replacement, and molecular pathways of the visual circuit. Moreover, rats have a better attention span compared with mice, which guarantee them superior candidates for complex visual and cognitive tasks necessary for behavioral assessment. Due to the advantage of size, rats allow more complex surgical procedures and sampling of blood and tissues, providing a more comprehensive testing of certain diseases. With these reasons, transgenic rat models have proven their unparalleled contribution to vision research in humans.

In addition to our developed *Pcp2-TdTomato* rat model, the CAG-LSL-TdTomato immunodeficient RD rats (RRRC strain #1055; *SD-Foxn1rnuTg((Rho-S334X)3,CAG-TdTomato)1010Mjsuc*) can be crossed with other *Cre*-expressing rat strains available from the RRRC (Rat Research Resource Center, University of Missouri), for example, *ChAT-Cre*,[34] *Pvalb-Cre*[35,36] or *Gad1*-Cre. Alternatively, rats can be injected intravitreally with viruses containing Cre in combination with cell-type specific promoters (e.g. *CamKII*, *c-fos*, or *synapsin*[32,37,38]) which will be useful to study connectivity of human stem-cell derived retinal or photoreceptor transplants. Our pilot experiments with retinal explants demonstrated that the *cre-lox* system can also be used in combination with *cre*-virus to achieve TdTomato label in the CAG-LSL-TdTomato (RNT) rat strain. We have submitted this strain to the RRRC so it is available for other researchers studying retinal transplantation and RD. Strain cryopreservation has now been completed (RRRC #1055).

Acknowledgments

The authors thank the UCI Transgenic Mouse facility for help with genotyping of the *foxn1* mutation. We also thank Michelle Y. Wu and the UCI Viral Core for their help with the virus experiments. We appreciate the technical assistance from staff and students of the Seiler lab: Samir Malhotra, Huong Do, Akashi Suon, Robert Sims, Meredith Liu, John Boutros, Quinn Tran, Jack Cho, Fiaza Ali, Irene Jin, Thuy-Lin Tran, Yuhan Chen, Umer Shahab, Jack Wang, Nevin V. Joseph, Cassidy Azores, and Renee Mercado.

Supported by NIH Grants R01EY031834 and R01EY032948, and UCI Department Ophthalmology bridge funds. This work was made possible, in part, through access to the Optical Biology Core Facility of the Developmental Biology Center, a shared resource supported by the Cancer Center Support Grant (CA-62203) and Center for Complex Biological Systems Support Grant (GM-076516) at the University of California, Irvine, California. We acknowledge support from NIH core grant P30 EY034070 and from an unrestricted grant from Research to Prevent Blindness to the Gavin Herbert Eye Institute at the University of California, Irvine, California.

Author Contributions: Designed the experiment: M.J.S., B.L., G.Z., and L.K.; Conducted the experiments: H.N., D.E., B.L., and G.Z.; Analyzed/interpreted data: M.J.S., H.N., D.E., B.L., G.Z., and L.K.; Provided materials: M.J.S. and L.K.; Wrote the article: M.J.S. and H.N.; Proofed/revised article: M.J.S., H.N., B.L., G.Z., and L.K.

Disclosure: **M.J. Seiler**, None; **H. Nguyen**, None; **D. Endejan**, Inotiv (E); **B. Lin**, None; **G. Zhao**, Inotiv, (E); **L. Klaskala**, Inotiv (E)

[*] MJS and HN contributed equally to this study and should be considered co-first authors.

References

1. Suleman N. Current understanding on retinitis pigmentosa: a literature review. *Front Ophthalmol (Lausanne)*. 2025;5:1600283.
2. Kamde SP, Anjankar A. Retinitis pigmentosa: pathogenesis, diagnostic findings, and treatment. *Cureus*. 2023;15:e48006.
3. Fleckenstein M, Schmitz-Valckenberg S, Chakravarthy U. Age-related macular degeneration: a review. *JAMA*. 2024;331:147–157.
4. Guymer RH, Campbell TG. Age-related macular degeneration. *Lancet*. 2023;401:1459–1472.
5. Confalonieri F, La Rosa A, Ottonelli G, et al. Retinitis pigmentosa and therapeutic approaches: a systematic review. *J Clin Med*. 2024;13:4680.
6. Yang J, Lewis GP, Hsiang CH, et al. Amelioration of photoreceptor degeneration by intravitreal transplantation of retinal progenitor cells in rats. *Int J Mol Sci*. 2024;25:8060.
7. Thomas BB, Rajendran Nair DS, Rahimian M, Hassan AK, Tran TL, Seiler MJ. Animal models for the evaluation of retinal stem cell therapies. *Prog Retin Eye Res*. 2025;106:101356.
8. LaVail MM, Nishikawa S, Steinberg RH, et al. Phenotypic characterization of P23H and S334ter rhodopsin transgenic rat models of inherited retinal degeneration. *Exp Eye Res*. 2018;167:56–90.
9. Thomas BB, Zhu D, Lin TC, et al. A new immunodeficient retinal dystrophic rat model for transplantation studies using human-derived cells. *Graefes Arch Clin Exp Ophthalmol*. 2018;256:2113–2125.
10. Seiler MJ, Aramant RB, Jones MK, Ferguson DL, Bryda EC, Keirstead HS. A new immunodeficient pigmented retinal degenerate rat strain to study transplantation of human cells without immunosuppression. *Graefes Arch Clin Exp Ophthalmol*. 2014;252:1079–1092.
11. Ishikura M, Muraoka Y, Hirami Y, Tu HY, Mandai M. Adaptive optics optical coherence tomography analysis of induced pluripotent stem cell-derived retinal organoid transplantation in retinitis pigmentosa. *Cureus*. 2024;16:e64962.
12. Liu YV, Santiago CP, Sogunro A, et al. Single-cell transcriptome analysis of xenotransplanted human retinal organoids defines two migratory cell populations of nonretinal origin. *Stem Cell Reports*. 2023;18:1138–1154.
13. Watari K, Yamasaki S, Tu HY, et al. Self-organization, quality control, and preclinical studies of human iPSC-derived retinal sheets for tissue-transplantation therapy. *Commun Biol*. 2023;6:164.
14. Tu HY, Watanabe T, Shirai H, et al. Medium- to long-term survival and functional examination of human iPSC-derived retinas in rat and primate models of retinal degeneration. *EBioMedicine*. 2019;39:562–574.
15. Sims R, Lin B, Xue Y, et al. Effect of immunosuppression on hESC-derived retina organoids in vitro and in vivo. *Stem Cell Res Ther*. 2025;16:165.
16. Lin B, Singh RK, Seiler MJ, Nasonkin IO. Survival and functional integration of human embryonic stem cell-derived retinal organoids after shipping and transplantation into retinal degeneration rats. *Stem Cells Dev*. 2024;33:201–213.
17. Thomas BB, Lin B, Martinez-Camarillo J-C, et al. Co-grafts of human embryonic stem cell derived retina organoids and retinal pigment epithelium for retinal reconstruction in immunodeficient retinal degenerate Royal College of Surgeons rats. *Front Neurosci*. 2021;15:752958.
18. Lin B, McLelland BT, Aramant RB, et al. Retina organoid transplants develop photoreceptors and improve visual function in RCS rats with RPE dysfunction. *Invest Ophthalmol Vis Sci*. 2020;61:34.
19. McLelland BT, Lin B, Mathur A, et al. Transplanted hESC-derived retina organoid sheets differentiate, integrate, and improve visual function in retinal degenerate rats. *Invest Ophthalmol Vis Sci*. 2018;59:2586–2603.
20. Xue Y, Lin B, Chen JT, Tang WC, Browne AW, Seiler MJ. The prospects for retinal organoids in treatment of retinal diseases. *Asia Pac J Ophthalmol (Phila)*. 2022;11:314–327.
21. Malhotra S, Seiler MJ, Browne AW. Challenges and advances in the production of transplantable retinal tissue from retinal organoids. *J Ophthalmic Vis Res*. 2025. doi:20:10.18502/jovr.v20.17499.
22. Cowan CS, Renner M, De Gennaro M, et al. Cell types of the human retina and its organoids at single-cell resolution. *Cell*. 2020;182:1623–1640 e1634.
23. Yamasaki S, Tu HY, Matsuyama T, et al. A Genetic modification that reduces ON-bipolar cells in hESC-derived retinas enhances functional integration after transplantation. *iScience*. 2022;25:103657.
24. Zhang XM, Chen BY, Ng AH, et al. Transgenic mice expressing Cre-recombinase specifically in retinal rod bipolar neurons. *Invest Ophthalmol Vis Sci*. 2005;46:3515–3520.

25. Lu Q, Ivanova E, Ganjawala TH, Pan ZH. Cre-mediated recombination efficiency and transgene expression patterns of three retinal bipolar cell-expressing Cre transgenic mouse lines. *Mol Vis*. 2013;19:1310–1320.
26. Murenu E, Pavlou M, Richter L, et al. A universal protocol for isolating retinal ON bipolar cells across species via fluorescence-activated cell sorting. *Mol Ther Methods Clin Dev*. 2021;20:587–600.
27. Lois C, Hong EJ, Pease S, Brown EJ, Baltimore D. Germline transmission and tissue-specific expression of transgenes delivered by lentiviral vectors. *Science*. 2002;295:868–872.
28. Seiler MJ, Lin RE, McLelland BT, et al. Vision recovery and connectivity by fetal retinal sheet transplantation in an immunodeficient retinal degenerate rat model. *Invest Ophthalmol Vis Sci*. 2017;58:614–630.
29. Prusky GT, West PW, Douglas RM. Behavioral assessment of visual acuity in mice and rats. *Vision Res*. 2000;40:2201–2209.
30. Douglas RM, Alam NM, Silver BD, McGill TJ, Tschetter WW, Prusky GT. Independent visual threshold measurements in the two eyes of freely moving rats and mice using a virtual-reality optokinetic system. *Vis Neurosci*. 2005;22:677–684.
31. Kim H, Kim M, Im SK, Fang S. Mouse Cre-LoxP system: general principles to determine tissue-specific roles of target genes. *Lab Anim Res*. 2018;34:147–159.
32. Shcholok T, Eftekharpour E. Cre-recombinase systems for induction of neuron-specific knockout models: a guide for biomedical researchers. *Neural Regen Res*. 2023;18:273–279.
33. Kawaharada K, Kawamata M, Ochiya T. Rat embryonic stem cells create new era in development of genetically manipulated rat models. *World J Stem Cells*. 2015;7:1054–1063.
34. Witten IB, Steinberg EE, Lee SY, et al. Recombinase-driver rat lines: tools, techniques, and optogenetic application to dopamine-mediated reinforcement. *Neuron*. 2011;72:721–733.
35. Wright AM, Zapata A, Hoffman AF, et al. Effects of withdrawal from cocaine self-administration on rat orbitofrontal cortex parvalbumin neurons expressing Cre recombinase: sex-dependent changes in neuronal function and unaltered serotonin signaling. *eNeuro*. 2021;8:ENEURO.0017-21.2021.
36. Patrono E, Hruzova K, Svoboda J, Stuchlik A. The role of optogenetic stimulations of parvalbumin-positive interneurons in the prefrontal cortex and the ventral hippocampus on an acute MK-801 model of schizophrenia-like cognitive inflexibility. *Schizophr Res*. 2023;252:198–205.
37. Kawabata H, Konno A, Matsuzaki Y, et al. Improving cell-specific recombination using AAV vectors in the murine CNS by capsid and expression cassette optimization. *Mol Ther Methods Clin Dev*. 2024;32:101185.
38. Juttner J, Szabo A, Gross-Scherf B, et al. Targeting neuronal and glial cell types with synthetic promoter AAVs in mice, non-human primates and humans. *Nat Neurosci*. 2019;22:1345–1356.
39. Molday RS, MacKenzie D. Monoclonal antibodies to rhodopsin: characterization, cross-reactivity, and application as structural probes. *Biochemistry*. 1983;22:653–660.
40. Rao DM, Horton ER, Barrington CL, et al. Systematic identification and characterization of eukaryotic and viral 2A peptide-bond-skipping sequences. *Cell Rep*. 2025;44:115822.

translational vision science & technology